

Recent Progress in Basis Light-front Quantization

Xingbo Zhao,^{*} Kaiyu Fu,[§] Hengfei Zhao,[†] Jiangshan Lan,^{**} Chandan Mondal,^{§§} Siqi Xu,[‡]

*Institute of Modern Physics, Chinese Academy of Sciences, Lanzhou 730000, China
School of Nuclear Science and Technology, University of Chinese Academy of Sciences, Beijing 100049, China*

^{*}E-mail: xbzhao@impcas.ac.cn, [§]E-mail: kaiyufu@impcas.ac.cn

[†]E-mail: zhaohengfei@impcas.ac.cn, ^{**}E-mail: jiangshanlan@impcas.ac.cn

^{§§}E-mail: mondal@impcas.ac.cn, [‡]E-mail: xsq234@impcas.ac.cn

James P. Vary

*Department of Physics and Astronomy, Iowa State University,
Ames, IA 50011, USA
E-mail: jvary@iastate.edu
(BLFQ Collaboration)*

Basis Light-front Quantization (BLFQ) is a nonperturbative approach to quantum field theory. In this paper, we report our recent progress in applying BLFQ to the positronium system in QED and to the meson and the baryon system in QCD. We present preliminary results on the mass spectrum, light-front wave functions and other observables of these systems, where one dynamical gauge boson is retained for the positronium and meson systems.

Keywords: Light-front quantization; positronium; meson; baryon

1. Introduction

Basis Light-front Quantization (BLFQ) has been developed as a nonperturbative approach to relativistic bound states¹. It is based on the Hamiltonian formalism and the light-front quantum field theory. In BLFQ, the bound state problem is cast into an eigenvalue problem of the Hamiltonian:

$$P^-|\beta\rangle = P_\beta^-|\beta\rangle, \quad (1)$$

where the eigenvalues P_β^- correspond to the mass spectrum and the eigenvectors $|\beta\rangle$ encode their structural information. In this paper, we report our recent progress in applying BLFQ to the positronium system in QED and the meson and baryon system in QCD.

2. Positronium

The positronium (“Ps”) is arguably the simplest bound state system in QED. In this work, we solve the positronium system from first principles - the QED Lagrangian². In order to make the numerical calculation feasible, we perform basis truncation by retaining the two leading Fock sectors, that is, $|\text{Ps}\rangle = a|e^+e^-\rangle + b|e^+e^-\gamma\rangle$. In addition, we truncate the basis in the transverse (longitudinal) direction with the truncation parameter N_{max} (K)¹. Larger N_{max} (K) translates to more complete bases in the transverse (longitudinal) direction. We obtain our light-front QED Hamiltonian from the QED Lagrangian via the Legendre transformation. In our truncated basis the light-front QED Hamiltonian, using light-front gauge, takes the following form,

$$P_{\text{QED}}^- = \int d^2x^\perp dx^- \frac{1}{2} \bar{\Psi} \gamma^+ \frac{m_{e0}^2 + (i\partial^\perp)^2}{i\partial^+} \Psi + \frac{1}{2} A^j (i\partial^\perp)^2 A^j + e j^\mu A_\mu + \frac{e^2}{2} j^+ \frac{1}{(i\partial^+)^2} j^+, \quad (2)$$

where ψ and A_μ are the fermion and gauge boson field operators, respectively, and $j^\mu = \bar{\Psi} \gamma^\mu \Psi$. The first two terms are their corresponding kinetic terms and the remaining terms describe their interaction. m_{e0} is the bare fermion mass. For numerical convenience, we take an artificially increased electromagnetic coupling constant $\alpha = 0.075$.

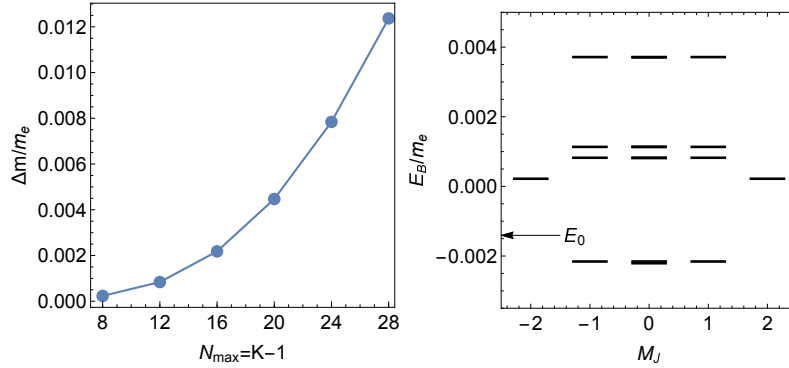


Fig. 1. Left panel: representative value of the mass counterterm (in units of the physical electron mass m_e) in the positronium problem as a function of basis truncation parameters $N_{\text{max}} = K - 1$; right panel: the binding energy (E_B) spectrum of the positronium system at $N_{\text{max}} = K - 1 = 28$ and $\alpha = 0.075$. E_0 is the ground state (1^1S_0) binding energy from nonrelativistic quantum mechanics with perturbative corrections.

In this calculation, we adopt the Fock-sector dependent renormalization³⁻⁵, according to which only the fermion mass in the $|e^+e^- \rangle$ sector needs to be renormalized, namely, the bare mass m_{e0} is different from the physical mass m_e . Different basis states take distinct values for the mass counterterm depending on their respective quanta available for self-energy fluctuation. The mass counterterms are determined from solving a series of single electron systems in the $|e \rangle + |e\gamma \rangle$ Fock sectors⁶.

The value of the mass counterterm $\Delta m = m_{e0} - m_e$ for a representative basis state in the positronium problem as a function of the truncation parameters is shown in the left panel of Fig. 1 and in the right panel, we present the binding energy spectrum of the positronium system, $E_B \equiv M_{Ps} - 2m_e$, for different spin projections M_J . The arrow indicates the value of the ground state binding energy from nonrelativistic quantum mechanics⁷, which is close to our result. We note that the mass counterterm is typically on a larger scale than that of the binding energy. We also note that the scale of the binding energy and structures of multiplets in the spectrum are in reasonable agreement with the previous calculation based on an effective one-photon-exchange interaction between the e^+ and e^- ⁸. The approximate degeneracy among different M_J substates and the information from the mirror parity and charge parity¹⁰ allow us to identify the low-lying eigenstates. For the $M_J = 0$ states, from bottom to up, the lowest six states are 1^1S_0 , 1^3S_1 , 2^1S_0 , 2^3S_1 , 2^3P_0 , and 2^3P_1 . Fig. 2 illustrates the light-front wave function (LFWF) in the $|e^+e^- \rangle$ sector for three low-lying states with $M_J = 0$. Their shape and nodal structures are qualitatively similar to those based on the one-photon-exchange effective interaction⁸.

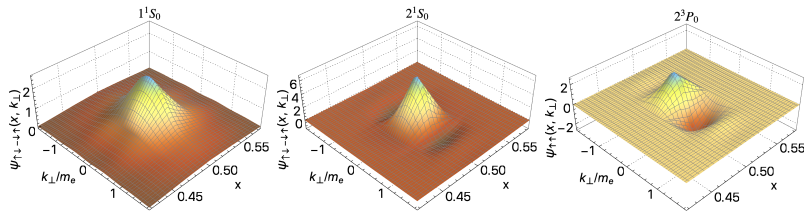


Fig. 2. The (normalized) LFWFs for the dominant spin component in the $|e^+e^- \rangle$ sector of the positronium system at $N_{\max} = K - 1 = 28$ and $\alpha = 0.075$. x is the longitudinal momentum fraction and k_\perp represents the relative transverse momentum between e^+ and e^- .

3. Heavy meson

A similar calculation can be carried over to the heavy meson system in QCD. Like the positronium system, we retain the lowest two Fock sectors, $|q\bar{q}\rangle$ and $|q\bar{q}g\rangle$, in our basis. Our Hamiltonian contains two parts. From the QCD Lagrangian, we obtain the first part of the Hamiltonian⁹, P_{QCD}^- , which in our truncated Fock space takes a similar form to the QED Hamiltonian, P_{QED}^- , in Eq. (2), with the fermion field Ψ identified as the quark field, the gauge boson field A_μ identified as the gluon field $A_\mu^a T^a$ and the electric charge e replaced by the color charge g . In order to achieve a more accurate reproduction of the meson mass spectrum, we allow the quark mass appearing in the quark-gluon vertex interaction, $gj^\mu A_\mu^a T^a$, to be an independent phenomenological parameter, m'_q , from m_q in the kinetic energy term. We also apply a nonzero gluon mass m_g to ensure the low-lying states are dominated by the $|q\bar{q}\rangle$ sector.

In addition we include a phenomenological confining potential¹⁰ in both the longitudinal and transverse directions in the $|q\bar{q}\rangle$ sector, which takes the following form,

$$P_C^- P^+ = \kappa^4 \vec{\zeta}_\perp^2 - \frac{\kappa^4}{(m_q + m_{\bar{q}})^2} \partial_x (x(1-x) \partial_x), \quad (3)$$

where x is the longitudinal momentum fraction of the quark⁸. $\vec{\zeta}_\perp \equiv \sqrt{x(1-x)} \vec{r}_\perp$ is the holographic variable introduced by Brodsky and de Téramond¹¹, and $\partial_x f(x, \vec{\zeta}_\perp) = \partial f(x, \vec{\zeta}_\perp) / \partial x|_{\vec{\zeta}_\perp}$. κ is the strength of the confinement and $m_q(m_{\bar{q}})$ is the mass of the quark (anti-quark). Thus, our total Hamiltonian is $P^- = P_{\text{QCD}}^- + P_C^-$.

With the charm quark mass $m_c = 1.561$ GeV (kinetic), $m'_c = 4.343$ GeV (interaction), the gluon mass $m_g = 0.4$ GeV, the confining strength $\kappa = 1.14$ GeV and the strong coupling constant $g = 2.3$ for the charmonium, and similarly the bottom quark mass $m_b = 4.767$ GeV (kinetic), $m'_b = 15$ GeV (interaction), $m_g = 0.4$ GeV, $\kappa = 1.948$ GeV and $g = 1.6$ for the bottomonium, our resulting mass spectra for the low-lying $c\bar{c}$ and $b\bar{b}$ states agree with the experimental values reasonably well, as shown in the left and middle panel of Fig. 3, respectively. With the same parameter set used in the $c\bar{c}$ and $b\bar{b}$ systems we obtain the mass spectrum for the B_c system, as in the right panel of Fig. 3. In Fig. 4 we present the ground state LFWFs of the $c\bar{c}$, $b\bar{b}$ and B_c system in the $|q\bar{q}\rangle$ sector.

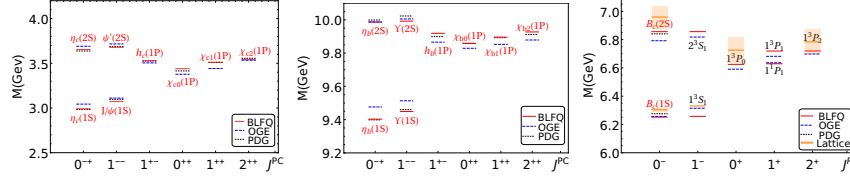


Fig. 3. Comparison of our BLFQ spectra at $N_{\max} = K - 1 = 8$ for charmonium (left), bottomonium (middle), and B_c meson (right) with the effective one-gluon-exchange (OGE) approach^{10,12} and the experimental values (PDG)¹³. Lattice results are from Ref.^{14–16}. The horizontal and vertical axes are the J^{PC} and invariant mass, respectively.

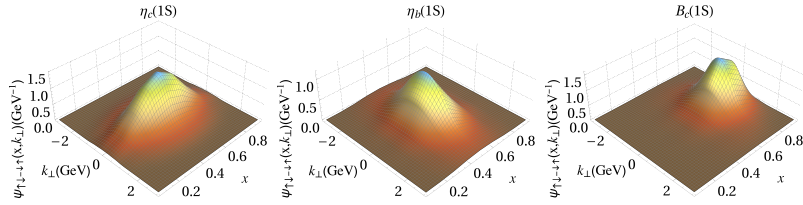


Fig. 4. The (normalized) LFWFs for the dominant spin component in the $|q\bar{q}\rangle$ sector of $\eta_c(1S)$ (left), $\eta_b(1S)$ (middle) and $B_c(1S)$ (right) at $N_{\max} = K - 1 = 8$. x is the longitudinal momentum fraction of the quark and k_{\perp} represents the relative transverse momentum between the quark and the anti-quark.

4. Light meson

We perform a similar calculation in the light meson sector. With $m_u = m_d = 0.33$ GeV, $m'_u = m'_d = 3.38$ GeV, $\kappa = 0.77$ GeV and $g=1.74$, we obtain the mass spectrum of the light mesons, as shown in the left panel of Fig. 5.

Although the masses for $a_0(980)$ and $b_1(1235)$ somewhat deviate from the experimental value¹³, the results for π , ρ , $a_1(1260)$, $\pi(1300)$, $a_2(1320)$, and $\pi_1(1400)$ are in good agreement with the experimental data¹³.

Next, we calculate the pion's parton distribution function (PDF), which represents the probability density of finding a parton with the longitudinal momentum fraction x inside the pion. We first calculate the initial scale PDF based on the LFWF from BLFQ in both the $|q\bar{q}\rangle$ and $|q\bar{q}g\rangle$ sectors. We then evolve the initial scale PDF from $\mu_0^2 = 0.31$ GeV² to the relevant experimental scales $\mu^2 = 16$ GeV² by the DGLAP equations^{17–19} using the higher order perturbative parton evolution toolkit²⁰.

In Fig. 5 (right panel), we compare our results with the E615 experimental result²¹ and the modified result of the E615 experiment²². We find

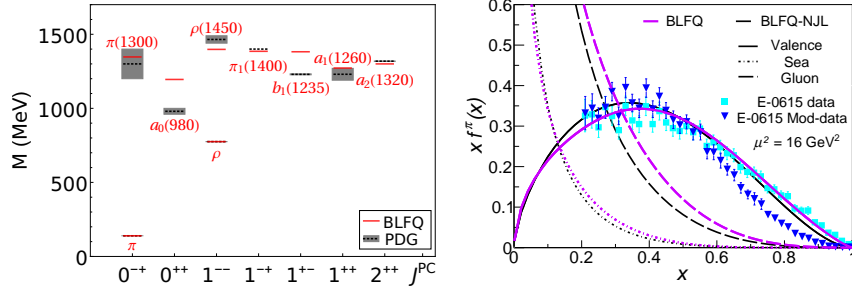


Fig. 5. Left panel: the mass spectrum of the light mesons; right panel: longitudinal momentum distribution $x f^{\pi}(x)$ as a function of longitudinal momentum fraction x of a parton in the pion.

that, for the valence PDF, our result shows slightly better agreement with the E615 experimental result²¹ in the high- x region compared to the earlier calculation based on an effective NambuJona-Lasinio interaction (BLFQ-NJL). For the gluon PDF, our result is larger than that obtained from the BLFQ-NJL model, and for the sea PDF, our result is close to that obtained from the BLFQ-NJL model²³.

5. Baryon

We perform an initial calculation of the baryon system based on an effective interaction in the $|qqq\rangle$ sector^{25,26}. This effective interaction consists of the (pairwise) one-gluon-exchange interaction and the (pairwise) longitudinal and transverse confining interactions. The parameters in the effective interaction are fixed by the mass and Dirac form factor of u, d flavor. For the baryon system, the ground state spin-1/2 (3/2) particle is the nucleon (Δ (1232)). Our preliminary results of their masses are compared with the experimental data in the left panel of Fig. 6. Our mass of Δ (1232) is about 170 MeV smaller than the experimental value. It remains to be seen that whether this mass discrepancy will decrease as the basis size increases. We also calculate the $I_{\frac{1}{2}, \frac{1}{2}}(Q^2)$ elastic form factor²⁷ of the proton and Δ^+ , which is compared in Fig 6. The larger slope of $I_{\frac{1}{2}, \frac{1}{2}}$ for Δ^+ at $Q^2 \rightarrow 0$ suggests that the charge radius of Δ^+ is larger than that of the proton, which is as expected since Δ^+ is an excitation of the proton.

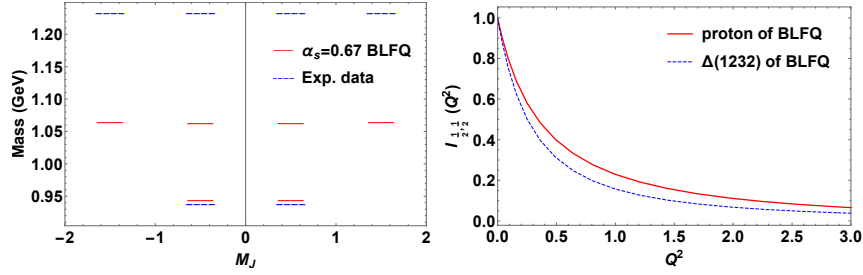


Fig. 6. Left panel: the masses of the nucleon and $\Delta(1232)$ compared to experimental data¹³; right panel: comparison of the $I_{\frac{1}{2}, \frac{1}{2}}(Q^2)$ elastic form factor between the proton and Δ^+ .

6. Conclusion

Through the applications to various bound state systems in QED and QCD we demonstrate that BLFQ is a versatile and powerful nonperturbative approach to quantum field theory for strongly interacting systems. We anticipate that in the future BLFQ will be a useful tool for understanding hadron mass spectrum and structure beyond the valence sector.

7. Acknowledgment

XZ is supported by Key Research Program of Frontier Sciences, CAS, Grant No ZDBS-LY-7020. CM is supported by the National Natural Science Foundation of China (NSFC) under the Grant No. 11850410436 and No. 11950410753. JPV is supported by the Department of Energy under Grants No. DE-FG02-87ER40371, and No. DE-SC0018223 (SciDAC4/NUCLEI). A portion of the computational resources were provided by the National Energy Research Scientific Computing Center (NERSC), which is supported by the Office of Science of the U.S. Department of Energy under Contract No.DE-AC02-05CH11231.

References

1. J. P. Vary *et al.*, Phys. Rev. C **81**, 035205 (2010).
2. K. Fu, H. Zhao, X. Zhao, J. P. Vary, to be published in the proceedings of Hadron 2019 conference (2020).
3. V. A. Karmanov, J.-F. Mathiot and A. V. Smirnov, Phys. Rev. D **77**, 085028 (2008).
4. V. A. Karmanov, J. F. Mathiot and A. V. Smirnov, Phys. Rev. D **86**, 085006 (2012).

5. X. Zhao, *Few Body Syst.* **56**, no. 6-9, 257 (2015).
6. X. Zhao, H. Honkanen, P. Maris, J. P. Vary and S. J. Brodsky, *Phys. Lett. B* **737**, 65 (2014).
7. H. A. Bethe and E. E. Salpeter, *Quantum Mechanics of One- and Two-Electron Atoms*, Springer, Heidelberg, 1957.
8. P. Wiecki, Y. Li, X. Zhao, P. Maris and J. P. Vary, *Phys. Rev. D* **91**, no. 10, 105009 (2015).
9. S. J. Brodsky, H. C. Pauli and S. S. Pinsky, *Phys. Rept.* **301**, 299 (1998).
10. Y. Li, P. Maris and J. P. Vary, *Phys. Rev. D* **96**, no. 1, 016022 (2017).
11. S. J. Brodsky, G. F. de Teramond, H. G. Dosch and J. Erlich, *Phys. Rept.* **584**, 1 (2015).
12. S. Tang, Y. Li, P. Maris and J. P. Vary, *Phys. Rev. D* **98**, no. 11, 114038 (2018).
13. M. Tanabashi *et al.* [Particle Data Group], *Phys. Rev. D* **98**, no. 3, 030001 (2018).
14. I. F. Allison *et al.* [HPQCD and Fermilab Lattice and UKQCD Collaborations], *Phys. Rev. Lett.* **94**, 172001 (2005).
15. E. B. Gregory *et al.*, *Phys. Rev. Lett.* **104**, 022001 (2010).
16. C. T. H. Davies, K. Hornbostel, G. P. Lepage, A. J. Lidsey, J. Shigemitsu and J. H. Sloan, *Phys. Lett. B* **382**, 131 (1996).
17. V. N. Gribov and L. N. Lipatov, *Sov. J. Nucl. Phys.* **15**, 438 (1972).
18. G. Altarelli and G. Parisi, *Nucl. Phys. B* **126**, 298 (1977).
19. Y. L. Dokshitzer, *Sov. Phys. JETP* **46**, 641 (1977).
20. G. P. Salam and J. Rojo, *Comput. Phys. Commun.* **180**, 120 (2009).
21. J. S. Conway *et al.*, *Phys. Rev. D* **39**, 92 (1989).
22. C. Chen, L. Chang, C. D. Roberts, S. Wan and H. S. Zong, *Phys. Rev. D* **93**, no. 7, 074021 (2016).
23. J. Lan, C. Mondal, S. Jia, X. Zhao and J. P. Vary, *Phys. Rev. Lett.* **122**, no. 17, 172001 (2019).
24. C. Alexandrou, T. Korzec, T. Leontiou, J. W. Negele and A. Tsapalis, *PoS LATTICE* **2007**, 149 (2007).
25. C. Mondal, S. Xu, J. Lan, X. Zhao, Y. Li, D. Chakrabarti and J. P. Vary, arXiv:1911.10913 [hep-ph].
26. S. Xu, C. Mondal, J. Lan, X. Zhao and J. P. Vary, to be published in the proceedings of Hadron 2019 conference (2020).
27. L. Adhikari, Y. Li, X. Zhao, P. Maris, J. P. Vary and A. Abd El-Hady, *Phys. Rev. C* **93**, no. 5, 055202 (2016).